Title

Using susceptibility-weighted imaging to determine response to combined anti-angiogenic, cytotoxic, and radiation therapy in patients with glioblastoma multiforme†

Journal

Neuro-Oncology, 15(4)

ISSN

1522-8517

Authors

Lupo, Janine M
Essock-Burns, Emma
Molinaro, Annette M
et al.

Publication Date

2013-04-01

DOI

10.1093/neuonc/nos325

Peer reviewed

Neuro-Oncology 15(4):480–489, 2013.
doi:10.1093/neuonc/nos325
Advance Access publication February 7, 2013

Using susceptibility-weighted imaging to determine response to combined anti-angiogenic, cytotoxic, and radiation therapy in patients with glioblastoma multiforme†

Janine M. Lupo, Emma Essock-Burns, Annette M. Molinaro, Soonmee Cha, Susan M. Chang, Nicholas Butowski, and Sarah J. Nelson

Department of Radiology and Biomedical Imaging (J.M.L., E.E.-B., S.C., S.J.N.); Department of Neurosurgery (A.M.M., S.C., S.M.C., N.B.); Department of Epidemiology and Biostatistics (A.M.M.); Department of Bioengineering and Therapeutic Sciences, University of California, San Francisco, California (S.J.N.)

Background. The goal of this study was to investigate whether the amount of hypointense signal on susceptibility-weighted imaging within the contrast-enhancing lesion (%SWI-h) on the pretreatment scan could determine response in patients with newly diagnosed glioblastoma multiforme who received external beam radiation therapy with concomitant anti-angiogenic therapy (enzastaurin) and cytotoxic chemotherapy (temozolomide).

Methods. Twenty-five patients were imaged before therapy (postsurgical resection) and scanned serially every 2 months until progression. Standard clinical MR imaging and SWI were performed on a 3T scanner. %SWI-h was quantified for each patient's pretreatment scan. Time to progression and death were used to characterize patients into non-, immediate-, and sustained-response groups for both events. Cox proportional hazards models were used to assess the association between %SWI-h and both progression-free survival (PFS) and overall survival (OS). Classification and regression tree analysis were used to determine optimal cutoffs on which to split %SWI-h.

Results. For both death- and progression-based response categories, %SWI-h was significantly higher in sustained responders than in nonresponders. Cox model coefficients showed an association between %SWI-h and PFS and OS, both in univariate analysis (PFS: hazard ratio [HR] = 0.966, 95% confidence interval [CI] = 0.942–0.988; and OS: HR = 0.945, 95% CI = 0.915–0.976) and when adjusting for baseline KPS, age, sex, and resection extent (PFS: HR = 0.968, 95% CI = 0.940 –0.994; and OS: HR = 0.943, 95% CI = 0.908 –0.976). A cutoff value of 38.1% significantly differentiated patients into 2 groups based on censored OS and into non- and intermediate-response categories based on time to progression.

Conclusions. These early differences suggest that SWI may be able to predict which patients would benefit most from similar combination therapies and may assist clinicians in making important decisions about patient care.

Keywords: glioma, response to anti-angiogenic therapy, susceptibility-weighted imaging.

As gliomas grow and progress to higher grade, the vascular supply is no longer adequate to support the increasing metabolic demands of rapidly proliferating tumor cells.[1] Regional hypoxia then ensues, leading to the up-regulation of vasogenic endothelial growth factor (VEGF) and the promotion of new blood vessel formation from the existing vasculature, a phenomenon known as angiogenesis.[2–5] Newly formed tumor vasculature is often tortuous, dilated, and inefficient, because it lacks the complex structure of normal brain vasculature, which disrupts the integrity of the blood-brain barrier and results in increased endothelial permeability. One of the more promising approaches for treating patients with newly diagnosed high-grade glioma or recurrent low-grade glioma that has

Received September 10, 2012; accepted November 26, 2012.

†This work was presented in part at the 18th Annual Meeting of International Society of Magnetic Resonance in Medicine, Stockholm, Sweden, 2010; and at the 15th Annual Meeting of Society of Neuro-oncology, Montreal, Canada, 2010.

Corresponding Author: Janine M. Lupo, PhD Byers Hall UCSF, Box 2532, 1700 4th St., Ste. 303, San Francisco, CA 94158 (janine.lupo@ucsf.edu).

transformed into higher grade is to add an anti-angiogenic therapy to the standard approaches. Anti-angiogenic treatments not only inhibit the formation of new vasculature, but also may normalize the existing tumor vasculature[5] and influence the delivery of chemotherapeutic agents.

Currently, there are numerous anti-angiogenic agents being considered in clinical practice. Because of its accelerated Food and Drug Administration approval, the anti-angiogenic drug most commonly investigated in patients with brain tumors at present is bevacizumab, which is a monoclonal antibody that disrupts the VEGF pathway, induces a decrease in tumor vessel size, and results in a more normalized vascular network that has reduced permeability. This compound has now been used in a number of studies as both a single and combined agent, in upfront and recurrent settings.[6–17] The recent phase II trial of bevacizumab used alone and in combination with irinotecan reported dramatic improvement in 6-month progression-free survival (PFS) and a high response rate among patients with recurrent glioblastoma multiforme (GBM).[7] In addition to these and other initial investigations examining large molecule VEGF inhibitors, the majority of current ongoing phase II/III studies have transitioned to using small molecule kinase or integrin inhibitors, such as enzastaurin,[18–25] cediranib,[26–28] pazopanib,[29] sorafenib,[30] sunitinib,[31] and cilengitide.[32,33] The therapeutic regimens may include a combination of these therapies, often involve the concurrent prescription of non–anti-angiogenic treatments, and can be administered to both patients with newly diagnosed and recurrent disease. Initial results have suggested that these agents can prolong 6-month PFS, but the potential long-term benefits and impact on survival remain to be seen.

It has recently been proposed that the use of adjuvant anti-angiogenic therapy in combination with standard radio- and chemotherapy acts to normalize the tortuous tumor vasculature and improve delivery of chemotherapeutics and oxygen.[34,35] Enzastaurin (LY317615), a protein kinase C-beta inhibitor important in the induction of and signaling through the VEGF pathway, is one such anti-angiogenic agent that is currently under investigation for its potential as an adjuvant therapy for patients with newly diagnosed GBM.[6,18,20] It suppresses tumor growth through multiple mechanisms, which include direct suppression of tumor cell proliferation and the induction of tumor cell death, coupled with the indirect effect of suppressing tumor-induced angiogenesis, thereby decreasing tumor blood supply.[6] Although the most recent phase I and II studies have shown only slight improvements in the median PFS and OS in entire populations receiving enzastaurin, the characteristics of response are highly variable, with some patients surviving >2 years while receiving therapy, whereas others experience treatment failure almost immediately.[19,21–25,36] This possibility of differential sensitivity to enzastaurin based on a small subset of the study population who showed long-term response but similar steady-state drug levels as the rest of the population stresses the importance of the need for a means to both identify patients who are the best candidates for a given therapy regime and to derive new parameters that are capable of noninvasively predicting patterns of response to anti-angiogenic therapy.

Susceptibility-weighted imaging (SWI) is a powerful tool for high resolution imaging of the vasculature that has been shown to improve the diagnosis of brain tumors because of its unique and potentially valuable contrast that is not always present on conventional anatomical or perfusion-weighted images. The technique relies on the phase signal of a T2*-weighted image to amplify contrast between veins and brain tissue in the magnitude image. Higher field strength scanners (>3 Tesla) heighten this effect and can facilitate the acquisition of images with 500 μ in-plane resolution and full brain coverage in <7 min. Although the exact biological basis for the hypointensity observed on SWI images in the tumor region is still unclear, our preliminary observations of the phase signal and the location of SWI hyperintensity in relation to precontrast T1 hyperinensity indicate that it is not the result of calcification (which would have positive phase) or subacute hemorrhage (which would be hyperintense on T1-weighted images). SWI has highlighted heterogeneity in the contrast-enhancing lesion (CEL) and regions of elevated blood volume or blood-brain barrier compromise.[37–39]

Because hypointense signal on SWI images has been shown to reflect both vascularity and vascular integrity,[39] this contrast mechanism is expected to be advantageous both as a predictive biomarker in identifying likely responders to therapy and in assessing treatment effect and response for anti-angiogenic and radiotherapy. The goal of this study was to investigate whether the amount of hypointense signal on SWI images in the CEL on the postsurgery, pretreatment scan can determine response and outcome in patients with newly diagnosed GBM brain tumors who receive concomitant anti-angiogenic, cytotoxic, and radiation therapy.

Materials and Methods

Patient Population

Twenty-five patients with newly diagnosed grade IV glioma based on the World Health Organization (WHO) criteria from 1 September 2007 through 31 December 2008 were examined in this study. All patients had undergone surgical resection and were later treated with a standard 6-week cycle of external beam radiation therapy. A chemotherapy regimen that included temozolomide (75 mg/m^2 daily during radiotherapy and 200 mg/m^2 for 5 days every 28-day cycle after radiotherapy) and enzastaurin (250 mg daily) concurrent and adjuvant to radiation therapy was subsequently administered. Patients were imaged before beginning therapy (postsurgical resection) and scanned serially every 2 months until progression. Patient age ranged from 25 to 70 years, with a median age of 57 years. To be enrolled in the study, patients were required to have a Karnofsky performance score (KPS) of at least 60, and those who discontinued therapy because of

adverse effects were excluded from the study population. All patients provided informed consent in accordance with guidelines established by our Institutional Review Board.

MR Imaging Acquisition

Patients were imaged with SWI before therapy on a 3T GE scanner (GE Healthcare Technologies, Milwaukee, WI) with an 8-channel phased array receive coil (MRI Devices, Gainesville, FL). High-resolution T2*-weighted SWI was acquired using a 3D flow-compensated spoiled gradient echo (SPGR) sequence with TE/TR 28/56ms, flip 20°, 24 cm FOV, 512 × 144 image matrix with GRAPPA R = 2 plus 16 autocalibrating lines,[40] and an in-plane resolution of 0.5 × 0.5 mm. Standard clinical pre- and postcontrast T1-weighted SPGR images (TR = 8.86 ms, TE = 2.50 ms, matrix = 256 × 256, slice thickness = 1.5 mm, FOV = 24 × 24 cm, TI = 400 ms, flip angle = 15°) were also acquired for defining anatomic regions of interest.

Image Processing

After each examination, the images were transferred to a Linux workstation (Sun Microsystems, Mountain View, CA) for the postprocessing steps illustrated in Fig. 1. The SWI processing used a 72 × 72 Hanning filter, and the resulting phase mask was multiplied with the magnitude T2*-weighted image 4 times. A low-pass filter with edge completion was applied to the combined images and minimum intensity projections (mIPs) through 8 mm thick slabs were generated to obtain the final SWI images used for analysis. The precontrast T1-weighted SPGR images were registered to the SWI images through rigid body transformations that maximized the normalized mutual information,[41] and the resulting transformation was applied to the postcontrast T1 SPGR images. The CEL region was manually defined from the registered postcontrast T1 SPGR images. Any hyperintensity that was also present on the precontrast T1 images was assumed to be indicative of subacute blood products and excluded.

Two methods were used to segment the region of hypointensity on SWI images. The hypointense region was both delineated manually, based on visual inspection, and automatically thresholded, based on local histogram analysis in the CEL mask. The volume of SWI hypointensity (SWI-h) in the CEL was then calculated and expressed as a fraction of CEL volume, %SWI-h, for each patient's pretreatment scan. In the automatic thresholding method, local histogram analysis, as illustrated in Fig. 1, was used to define SWI hypointense voxels with intensity values <1.5 times the full-width half-max below the mode of the histogram. This automatic threshold deviated from the manually defined threshold by only 3.85 signal intensity units on average (range, 0.1%–19.8%) and was used in all analyses reported. After thresholding, 2 of the initial 27 patients in the dataset were excluded for having lesion sizes of <0.5 cc, which were too small to be reliably analyzed.

Definition of Response Categories

PFS was defined as the time from the pretherapy, baseline scan to the scan date of clinical progression, and

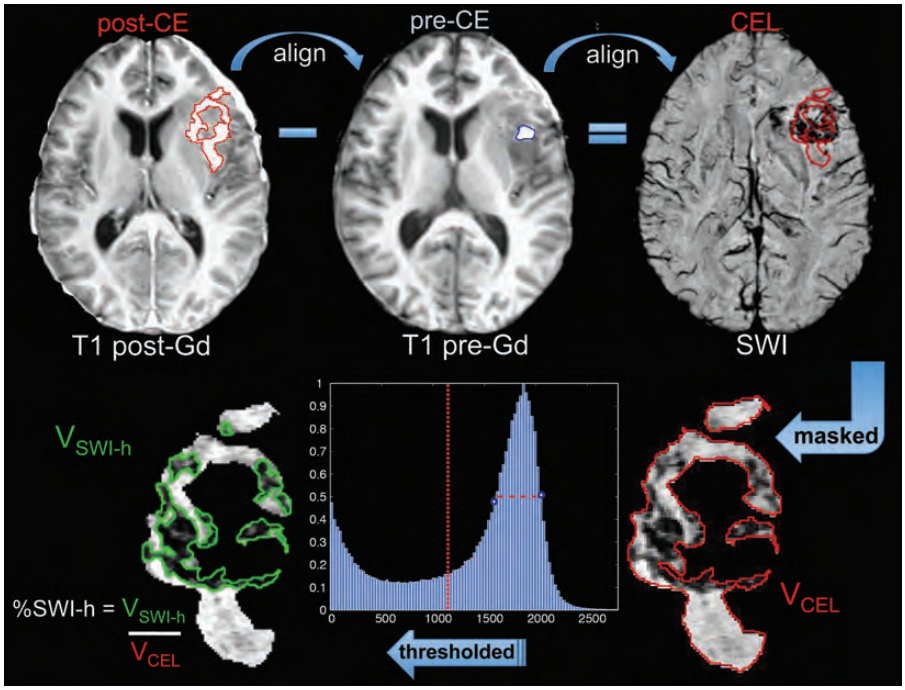

Fig. 1. Methods for alignment and calculation of %SWI-h parameter.

OS was the time from the baseline scan date until death. In the case of no progression or death, the event time was truncated and censored at 31 December 2010. Only 2 patients had not progressed, and 3 had not died by this date. To address the potential for pseudoprogression, the clinical histories of all patients who progressed within 12 weeks of the completion of radiotherapy and those of all patients with a suspect scan followed by stable disease were centrally re-reviewed by a neuro-oncologist. Notation was made regarding reoperation and location of recurrence to confirm true progression in accordance with the recommendations of Wen et al.[42] On the basis of this criteria, none of the patients included in this study exhibited pseudoprogression. As shown in Fig. 2B, patients were categorized into 1 of 3 response groups based on time of first progression and death: (1) nonresponders (progression: <6 months; death: <12 months), (2) intermediate responders (progression: 6–12 months; death: 12–18 months), and (3) sustained responders (progression: >12 months; death: >18 months). All censored patients were included in the sustained responder category, because they were censored after the truncation date.

Statistical Analysis

All statistical analyses were performed using R software, version 2.9.2 (www.r-project.org). A Wilcoxon rank-sum test was used to test for significant differences in %SWI-h values among response groups for both time to progression and death. A univariate Cox proportional hazards (CoxPH) model was used to assess the association between %SWI-h and both PFS and OS, landmarked from the date of the pretreatment scan. Multivariate CoxPH analysis was implemented to evaluate whether %SWI-h was predictive of PFS or OS when adjusted for the clinical factors of baseline KPS, age, sex, and extent of resection. Because of the exploratory nature of the study, no formal adjustment of type I error was undertaken; in all cases, $P < .05$ was considered to be statistically significant.

Classification and regression tree (CART) analysis was used to determine optimal cutoffs for %SWI-h on which to split data based on PFS, OS, and the response categories. For both outcome types (censored and categorical), only one split was found per tree based on 10-fold cross-validation. Survival trees were built using

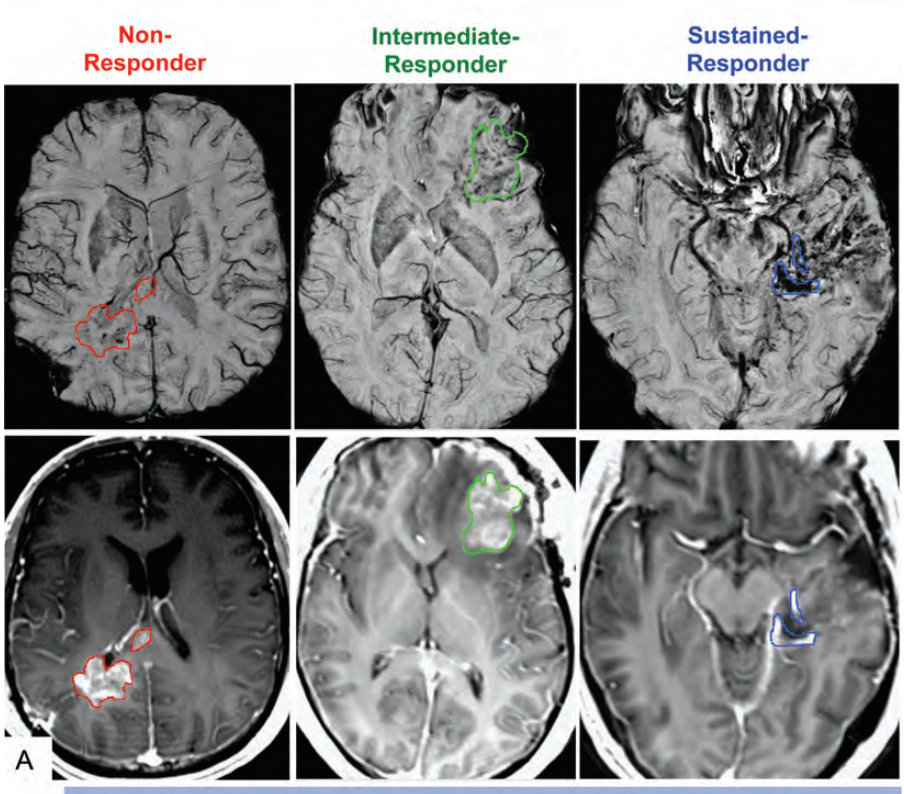

B

Response Category	Progression	Death
Non-Responder	≤6 months	≤12 months
Intermediate Responder	6–12 months	12–18 months
Sustained Responder	≥12 months	≥18 months

Fig. 2. (A) SWI with CEL contour overlay (top) and corresponding post-gad T1 images (bottom) for each response group. (B) Definition of response-based categories for time to progression and death.

the default survival method in the R package (rpart)[43] for PFS and OS, and the resulting split was assessed using univariate CoxPH models to obtain a hazard ratio and corresponding *P* value. For each combination of binary response outcomes, categorical trees were constructed and univariate logistic regression models were used to determine the odds ratio and corresponding *P* value for the resulting split.

Results

Response Categories Analysis

The spatial differences in the pattern of SWI-h among response groups can be visualized in Fig. 2. Sustained responders had hypointense signal on SWI images nearly throughout the entire CEL (Fig. 2A), whereas intermediate responders had a more speckled pattern of hypointense signal in this region (Fig. 2B). Nonresponders showed only a sparse amount of hypointense signal in the area of contrast enhancement (Fig. 2C). Although a trend was observed between CEL volume and time to death, no significant differences in CEL volumes were found among response groups for either event.

For both progression- and death-based response categories, the %SWI-h in the CEL was significantly larger in sustained responders than in nonresponders (66% vs 25% respective medians, $P = .008$ for progression; 48% vs. 12% respective medians, $P < .03$ for death), as shown in panel A of Figs 3 and 4. A significant increase in %SWI-h was also observed for intermediate responders, compared with nonresponders (41% vs. 25%; $P < .03$; Fig. 3A), when groups were formed on the basis of time to progression, and sustained responders, compared with intermediate responders (48% vs. 27%; $P < .02$; Fig. 4A), when grouping response based on time to death. Although trends were observed in the amount of SWI-h in the CEL with improved response between all groups for both events, the difference in SWI-h volume fraction between sustained and intermediate responders based on time to first progression and intermediate and nonresponders based on time to death did not reach statistical significance (Figs 3 and 4).

CoxPH Model Analysis for Early Prediction of Survival

Univariate CoxPH model coefficients showed a statistically significant association between %SWI-h and PFS ($r = 0.49$, $P < .007$), and OS ($r = 0.67$, $P < .0001$). A greater amount of %SWI-h indicated a more favorable prognosis (Figs 3 and 4). Each 1% increase in %SWI-h at baseline resulted in a 3.4% reduction in risk of progression (hazard ratio [HR] = 0.966; 95% confidence interval [CI] = 0.942–0.988) and 5.5% reduction in risk of death (HR = 0.945; 95% CI = 0.915–0.976). The CoxPH curves for PFS and OS for the 25 patients are shown in Figs 3 and 4. Adjusting for baseline KPS,

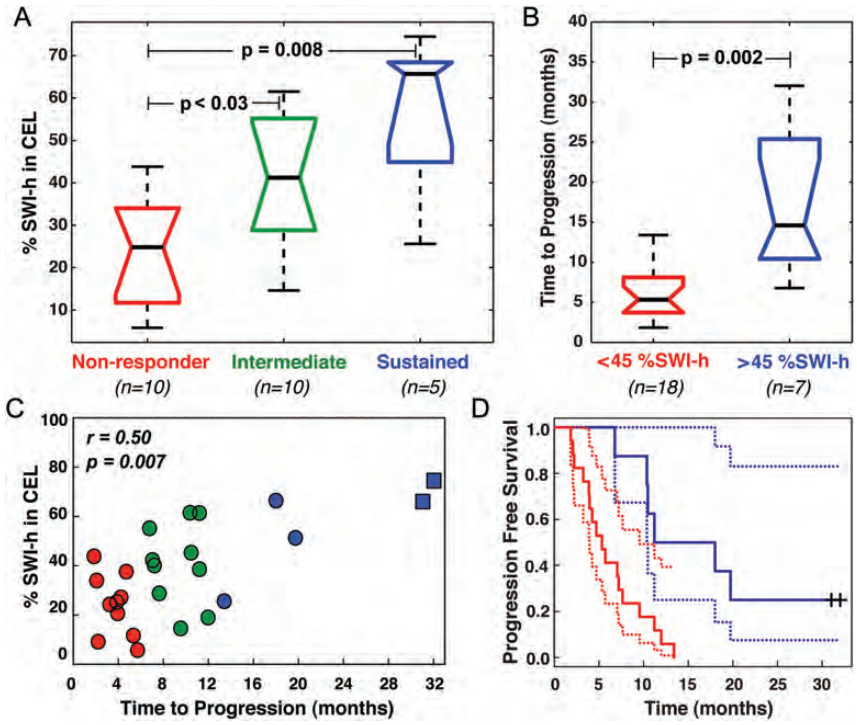

Fig. 3. PFS results. Boxplots of (A) %SWI-h for each response group and (B) when split on CART threshold for progression, including the 2 censored patients. (C) Relationship between %SWI-h and PFS. (D) CoxPH survival curves for each CART split group in B with %SWI-h < 45% in red, %SWI-h > 45% in blue, and the corresponding 95% confidence intervals indicated by dashed lines. □, + indicate have not progressed.

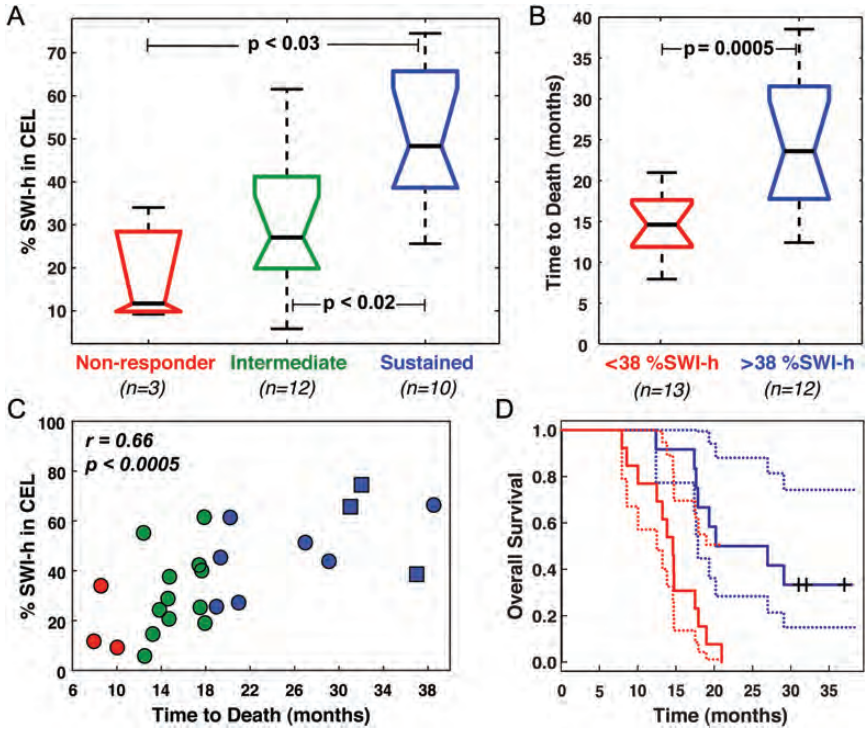

Fig. 4. OS results. Boxplots of (A) %SWI-h for each response group and (B) when split on CART threshold for death, including the 3 censored patients. (C) Relationship between %SWI-h and OS. (D) CoxPH survival curves for each CART split group in B, with %SWI-h < 38% in red, %SWI-h > 38% in blue, and the corresponding 95% confidence intervals indicated by dashed lines. □, + indicate are still alive.

age, sex, and extent of resection, multivariate Cox regression analysis showed that greater %SWI-h at baseline was still a protective factor for PFS (HR = 0.968; 95% CI = 0.940 −0.994; $P = .01$) and OS (HR = 0.943; 95% CI = 0.908 −0.976; $P = .0005$). Each 1% increase in %SWI-h at baseline resulted in a 3.2% reduction in risk of progression and 5.7% reduction in risk of death.

CART Analysis

The results of CART analysis are shown in Table 1 and Figs 3 and 4. Although a %SWI-h value of 44.6% was found to separate the patients into 2 groups based on censored PFS, a cutoff value of 38.1% significantly differentiated patients both into 2 groups, based on censored OS, and into non- and intermediate-responder categories, based on time to progression. In the latter binary analysis, the CART cutoff successfully classified 75% of the nonresponders and 87.5% of intermediate-responders. For the binary time to death CART analysis, a cutoff %SWI-h value of 43.1% effectively classified 77.8% of intermediate-responders and 76.9% of sustained-responders. The large odds ratios and low P values for both binary CART analyses emphasized the difference in risk between the 2 groups despite the wide CIs present because of the small number of patients. As expected based on the response categories analysis, no splits were found to distinguish either intermediate- and sustained-responders, based on time to progression, or non- and intermediate-responders, based on time to death, because no statistically significant group differences were found between these populations (Figs 2 and 3).

Discussion

Of critical importance in evaluating combinatory treatment strategies involving anti-angiogenic therapies is the availability of noninvasive imaging techniques that can directly and objectively assess their effectiveness in terms of both tumor burden and vascular patency. Ideally, the quantitative parameters derived from these imaging methods would determine which patients would benefit most from a given therapy before the onset of treatment and ultimately provide clinicians with a tool for identifying the best candidates for diverse therapeutic strategies. In this study, we successfully achieved the goal of identifying a predictive biomarker for one such form of antiangiogenic therapy, the PKC-kinase inhibitor, enzastaurin, using a parameter derived from SWI. To our knowledge, this is the first time SWI has been shown to predict outcome in a population of patients with brain tumors.

The parameter %SWI-h, or the fraction of hypointense signal on an SWI in the CEL lesion, was found to be predictive of both PFS and OS in patients with newly diagnosed GBM who were receiving a treatment

Table 1. Summary of CART analysis

Event	Cutoff value for event	N/node	Median event time/node (mo)	Hazard/Odds event	95% CI	*P* value
Progression						
All data ($N = 23$)[a]	44.6%	17/6	5.33/14.6	5.09 (HR)	1.66, 15.6	<.004
Non vs Intermediate ($N = 20$)[b]	38.1%	12/8	4.47/8.78	23.0 (OR)	2.4, 492	<.02
Intermediate vs Sustained ($N = 15$)[b]	–	–	–	–	–	–
Death						
All data ($N = 22$)[a]	38.1%	13/9	14.6/20.2	5.14 (HR)	1.86, 14.2	<.001
Non vs Intermediate ($N = 15$)[b]	–	–	–	–	–	–
Intermediate vs Sustained ($N = 22$)[b]	43.1%	9/13	17.4/21.0	11.7 (OR)	1.8, 116	<.02

Abbreviations: CI, confidence interval; HR, hazard ratio; OR, odds ratio.
[a]Statistical significance determined with CoxPH.
[b]Statistical significance determined with logistic regression.

regime consisting of upfront radiation therapy, temozolomide, and enzastaurin. There are 2 plausible underlying mechanisms to elucidate why a larger region of hypointensity on SWI in the core of the tumor would result in a better prognosis. The most likely explanation is that tumors with a larger extent of damaged vasculature initially are more likely to benefit from a treatment regimen containing an anti-angiogenic agent that aims to normalize the existing vasculature. The more abnormal vessels present, the greater the potential effect of the anti-angiogenic agent on pruning excess vessels and decreasing the oxygen supply to the tumor or fascilitating the delivery of chemotherapy, resulting in a heightened response and improved patient outcome. To test whether this is in fact the case, future studies evaluating the ability of baseline %SWI-h to predict outcome in patients with GBM who do not receive an anti-angiogenic agent are necessary. It is also possible that SWI hypointensity is reflecting the amount of chronic hemorrhage in the tumor (subacute hemorrhage, demarcated by hyperintensity on the precontrast injection T1-weighted image, was explicitly excluded from the contrast-enhancing tumor region). More chronic hemorrhage in the CEL would indicate less active tumor, which would, in turn, result in more favorable outcome measures. If the latter is the case, the type of therapy should not influence the ability of this parameter to predict prognosis. However, findings from the literature, whereby rapid functional vascular normalization both in terms of a reduction in vessel size and overall permeability derived from dynamic susceptibility-weighted contrast-enhanced and dynamic contrast-enhanced perfusion-weighted imaging were observed in patients with GBM who received other anti-angiogenic therapies,[26,34] support the former hypothesis.

In identifying robust prognostic markers from quantitative imaging metrics, the first step is to establish a relationship between the candidate parameter(s) and outcome measure. This was achieved for %SWI-h in the first section of the results, in which we showed that the %SWI-h in the CEL was significantly higher in sustained responders than in nonresponders for both time to progression and death. These differences did not exist for baseline CEL volume for either event. Univariate CoxPH models also demonstrated strong associations between %SWI-h and both PFS and OS. After a significant association is ascertained between the imaging marker and outcome measure, the relationship must also be demonstrated with high confidence when controlling for known clinical factors. Our data confirmed that an elevated %SWI-h value at baseline is a protective factor for both PFS and OS analyses, with highly significant hazard ratios. Nevertheless, the ultimate goal is to provide the clinician with a decision-making tool that can objectively determine whether a patient should be administered a given therapy (in this case, concomitant enzastaurin) based on their postsurgery, pretreatment baseline scan. To achieve this end, we implemented CART analysis to determine the optimal cutoff for deciding whether a patient is likely to benefit from anti-angiogenic therapy (in this case, enzastaurin). We found that %SWI-h best distinguished early progressors and long-term survivors, with values >38% significantly separating patients who benefited the most from enzasturin, according to both progression- and survival-based outcome measures.

Another strength of this study lies in the ability to use a quantitative measure, %SWI-h, to stratify patients noninvasively before any therapy administration, without having to wait for signs of response. Evaluating response to anti-angiogenic therapies using standard response criteria is often a challenge because of the apparent reduction in enhancing volume from transient normalization of the blood-brain barrier rather than antitumor activity. The vast majority of literature on predicting response to anti-angiogenic therapies, therefore, has focused on identifying early changes in physiological and metabolic imaging parameters that either more accurately reflect early antitumor activity of the therapeutic agent or later preclude any evidence of progression based on standard anatomical imaging. In several of these initial studies, response rate was used as the primary end point,[17,26,34] which has since been shown to correlate poorly with more

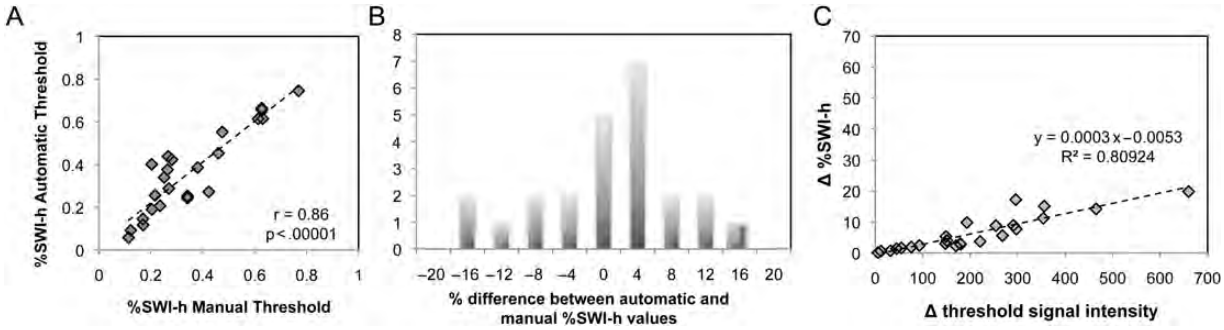

Fig. 5. Relationship between automatic and manual thresholding. In (A), scatter plot of %SWI-h values for automatic versus manual thresholding. In (B), histogram of percentage difference between %SWI-h derived from automatic and manual thresholding across all patients. In (C), change in %SWI-h between manual and automatic methods as a function of change in threshold intensity between methods. Larger differences in thresholds resulted in greater changes in the %SWI-h parameter, with a maximum deviation of 20%.

stable outcome measures, such as PFS and OS.[22,44] The VEGF-targeting class of drugs in particular result in even higher pseudo response rates, compared with historical controls[6–8,26] with only marginal improvements, if any, in survival, despite the somewhat delayed onset of progression.[9–11,25,30] Our results consistently indicated that %SWI-h was more associated with OS than with PFS. This is advantageous in the current context in which the vasogenic effect of anti-angiogenic therapies often masks the presence of active tumor cells, and extended PFS does not necessarily reflect overall patient outcome, because after progression, the rate of decline often hastens and the time from progression to death is reduced.

Despite the promising impact of our findings on patient treatment, there are some potential limitations that need to be addressed. The disadvantage of using categorical response assessment is that it does not provide a continuous scale on which to measure response and to test predictive hypotheses. Although the use of RANO criteria to evaluate PFS is still limited in the evaluation of response to anti-angiogenic therapy,[45] it does provide a scale for evaluating early biomarkers. While OS is likely to be a more appropriate end point in evaluating response to anti-angiogenic therapy, it is still limited by the influence of salvage treatments.[45] The advantage in integrating the discrete categorical radiographic assessment of response with the continuous PFS and OS scales is that this type of analysis facilitates elucidating differences in SWI hypointensity that could accurately identify radiographic response groups and predict outcome. Despite the distinct contrast present on the SWI images, the other main source of variability in this study arises from inaccuracies of thresholding the projected SWI images, as shown in Fig. 5. However, this error was minimized using an automatic technique in which 65% of the patients exhibited variations of %SWI-h of $<5\%$ between methods (Fig. 5B). The 2 techniques were also highly correlated with a correlation coefficient of .86 ($P < .001$, Spearman Rank correlation) (Fig. 5A), with larger differences in thresholds between methods resulting in greater changes in the %SWI-h parameter (Fig. 5C). Although the results reported in this article used the automatic method to remove user bias, varying the threshold had little effect on the volumes of SWI-h, and all the same findings were observed when using the visually defined thresholds.

In conclusion, the volume of SWI hypointensity in the CEL pretherapy was associated with both PFS and OS. These findings suggest that tumors with a larger extent of hypointense signal on SWI initially are more likely to benefit from a treatment regimen containing concomitant anti-angiogenic, cytotoxic, and radiation therapy. The ability to stratify patients on the basis of quantitative measures obtained noninvasively before therapy can aid in identifying patients who are the best candidates for different therapeutic strategies. Future studies will validate these results in other patient populations receiving alternate anti-angiogenic treatment regimens, investigate the patterns of SWI-h before progression, and incorporate functional imaging changes derived from perfusion- and diffusion-weighted imaging.

Acknowledgments

We thank Adam Elkhaled, Trey Jalbert, Bert Jimenez, Mary McPolin, Jason Crane, and Beck Olson of the Department of Radiology and Biomedical Imaging at UCSF, for their assistance with postprocessing issues, scanning, and data collection.

Funding

This study was supported by UC Discovery academic-industry partnership grants (LSIT01-10107 and ITL-BIO04-10148) in conjunction with GE Healthcare, National Institutes of Health (grants R01-CA059880 and P50-CA97257), and a Joelle Syverson American Brain Tumor Association Fellowship.

References

1. Folkman J. The role of angiogenesis in tumor growth. *Semin Cancer Biol*. 1992;3(2):65–71.
2. Amoroso A, Del Porto F, Di Monaco C, Manfredini P, Afeltra A. Vascular endothelial growth factor: a key mediator of neoangiogenesis. A review. *Eur Rev Med Pharmacol Sci*. 1997;1(1–3):17–25.
3. Brat DJ, Van Meir EG. Glomeruloid microvascular proliferation orchestrated by VPF/VEGF: a new world of angiogenesis research. *Am J Pathol*. 2001;158(3):789–796.
4. Damert A, Machein M, Breier G, et al. Up-regulation of vascular endothelial growth factor expression in a rat glioma is conferred by two distinct hypoxia-driven mechanisms. *Cancer Res*. 1997;57(17): 3860–3864.
5. Wesseling P, Ruiter DJ, Burger PC. Angiogenesis in brain tumors; pathobiological and clinical aspects. *J Neurooncol*. 1997;32(3):253–265.
6. Vredenburgh JJ, Desjardins A, Herndon JE, et al. Phase II trial of bevacizumab and irinotecan in recurrent malignant glioma. *Clin Cancer Res*. 2007;13:1253–1259.
7. Friedman HS, Prados MD, Wen PY, et al. Bevacizumab alone and in combination with irinotecan in recurrent glioblastoma. *J Clin Oncol*. 2009;27:4733–4740.
8. Kreisl TN, Kim L, Moore K, et al. Phase II trial of single-agent bevacizumab followed by bevacizumab plus irinotecan at tumor progression in recurrent glioblastoma. *J Clin Oncol*. 2009;27:740–745.
9. Hofer S, Elandt K, Greil R, et al. Clinical outcome with bevacizumab in patients with recurrent high-grade glioma treated outside clinical trials. *Acta Oncol*. 2011;50(5):630–635.
10. Lai A, Tran A, Nghiemphu PL, et al. Phase II study of bevacizumab plus temozolomide during and after radiation therapy for patients with newly diagnosed glioblastoma multiforme. *J Clin Oncol*. 2011; 29(2):142–148.
11. Sathornsumetee S, Desjardins A, Vredenburgh JJ, et al. Phase II trial of bevacizumab and erlotinib in patients with recurrent malignant glioma. *Neuro Oncol*. 2010;12(12):1300–1310.
12. Hasselbalch B, Eriksen JG, Broholm H, et al. Prospective evaluation of angiogenic, hypoxic and EGFR-related biomarkers in recurrent glioblastoma multiforme treated with cetuximab, bevacizumab and irinotecan. *APMIS*. 2010;118(8):585–594.
13. Raizer JJ, Grimm S, Chamberlain MC, et al. A phase 2 trial of single-agent bevacizumab given in an every-3-week schedule for patients with recurrent high-grade gliomas. *Cancer*. 2010;116(22):5297–5305.
14. Thompson EM, Dosa E, Kraemer DF, Neuwelt EA. Treatment with bevacizumab plus carboplatin for recurrent malignant glioma. *Neurosurgery*. 2010;67(1):87–93.
15. Francesconi AB, Dupre S, Matos M, et al. Carboplatin and etoposide combined with bevacizumab for the treatment of recurrent glioblastoma multiforme. *J Clin Neurosci*. 2010;17(8):970–974.
16. Hasselbalch B, Lassen U, Hansen S, et al. Cetuximab, bevacizumab, and irinotecan for patients with primary glioblastoma and progression after radiation therapy and temozolomide: a phase II trial. *Neuro Oncol*. 2010;12(5):508–516.
17. Pope WB, Xia Q, Paton VE, et al. Patterns of progression in patients with recurrent glioblastoma treated with bevacizumab. *Neurology*. 2011;76(5):432–437.
18. Butowski N, Chang SM, Lamborn KR, et al. Enzastaurin plus temozolomide with radiation therapy in glioblastoma multiforme: a phase I study. *Neuro Oncol*. 2010;12(6):608–613.
19. Kreisl TN, Kotliarova S, Butman JA, et al. A phase I/II trial of enzastaurin in patients with recurrent high-grade gliomas. *Neuro Oncol*. 2010; 12(2):181–189.
20. Teicher BA, Alvarez E, Menon K, et al. Antiangiogenic effects of a protein kinase Cbeta-selective small molecule. *Cancer Chemother Pharmacol*. 2002;49:69–77.
21. Chen YB, LaCasce AS. Enzastaurin. *Expert Opin Investig Drugs*. 2008;17:939–944.
22. Tabatabai G, Frank B, Wick A, et al. Synergistic antiglioma activity of radiotherapy and enzastaurin. *Ann Neurol*. 2007;61:153–161.
23. Robertson MJ, Kahl BS, Vose JM, et al. Phase II study of enzastaurin, a protein kinase C beta inhibitor, in patients with relapsed or refractory diffuse large B-cell lymphoma. *J Clin Oncol*. 2007;25:1741–1746.
24. Wick W, Puduvalli VK, Chamberlain MC, et al. Phase III study of enzastaurin compared with lomustine in the treatment of recurrent intracranial glioblastoma. *J Clin Oncol*. 2010;28(7):1168–1174.
25. Butowski N, Chang SM, Lamborn KR, et al. Phase II and pharmacogenomics study of enzastaurin plus temozolomide during and following radiation therapy in patients with newly diagnosed glioblastoma multiforme and gliosarcoma. *Neuro Oncol*. 2011;13(12):1331–1338.
26. Batchelor TT, Sorensen AG, di Tomaso E, et al. AZD2171, a pan-VEGF receptor tyrosine kinase inhibitor, normalizes tumor vasculature and alleviates edema in glioblastoma patients. *Cancer Cell*. 2007;11: 83–95.
27. Norden AD, Drappatz J, Muzikansky A, et al. An exploratory survival analysis of anti-angiogenic therapy for recurrent malignant glioma. *J Neurooncol*. 2009;92(2):149–155.
28. Batchelor TT, Duda DG, di Tomaso E, et al. Phase II study of cediranib, an oral pan-vascular endothelial growth factor receptor tyrosine kinase inhibitor, in patients with recurrent glioblastoma. *J Clin Oncol*. 2010; 28(17):2817–2823.
29. Iwamoto FM, Lamborn KR, Robins HI, et al. Phase II trial of pazopanib (GW786034), an oral multi-targeted angiogenesis inhibitor, for adults with recurrent glioblastoma (North American Brain Tumor Consortium Study 06-02). *Neuro Oncol*. 2010;12(8):855–861.
30. Hainsworth JD, Ervin T, Friedman E, et al. Concurrent radiotherapy and temozolomide followed by temozolomide and sorafenib in the first-line treatment of patients with glioblastoma multiforme. *Cancer*. 2010; 116(15):3663–3669.
31. Neyns B, Sadones J, Chaskis C, et al. Phase II study of sunitinib malate in patients with recurrent high-grade glioma. *J Neurooncol*. 2011;103(3): 491–501.
32. Reardon DA, Fink KL, Mikkelsen T, et al. Randomized phase II study of cilengitide, an integrin-targeting arginine-glycine-aspartic acid peptide, in recurrent glioblastoma multiforme. *J Clin Oncol*. 2008;26(34): 5610–5617.
33. Stupp R, Hegi ME, Neyns B, et al. Phase I/IIa study of cilengitide and temozolomide with concomitant radiotherapy followed by cilengitide and temozolomide maintenance therapy in patients with newly diagnosed glioblastoma. *J Clin Oncol*. 2010;28(16):2712–2718.
34. Jain RK. Normalizing tumor vasculature with anti-angiogenic therapy: a new paradigm for combination therapy. *Nat Med*. 2001;7:987–989.
35. Jain RK, Tong RT, Munn LL. Effect of vascular normalization by antiangiogenic therapy on interstitial hypertension, peritumor edema, and lymphatic metastasis: insights from a mathematical model. *Cancer Res*. 2007;67:2729–2735.

36. Essock-Burns E, Lupo JM, Cha S, et al. Assessment of perfusion MRI-derived parameters in evaluating and predicting response to anti-angiogenic therapy in patients with newly diagnosed glioblastoma. *Neuro Oncol*. 2011;13(1):119–131.
37. Lupo JM, Lee MC, Cha S, Chang SM, Nelson SJ. Imaging blood vessel volume in high grade gliomas at 3T using susceptibility-weighted imaging and dynamic susceptibility contrast perfusion MRI [abstract]. Proceedings of the 14th Annual Meeting of the International Society for Magnetic Resonance in Medicine; 8–12 May, 2006.
38. Park MJ, Kim HS, Jahng GH, Ryu CW, Park SM, Kim SY. Semi-quantitative assessment of intratumoral susceptibility signals using non-contrast-enhanced high-field high-resolution susceptibility-weighted imaging in patients with gliomas: comparison with MR perfusion imaging. *AJNR Am J Neuroradiol*. 2009;30(7):1402–1408.
39. Lupo JM, Chang SM, Nelson SJ. Using 7T susceptibility-weighted imaging to aid in the characterization of high-grade gliomas [abstract]. Proceedings of the 16th Annual Meeting of the International Society for Magnetic Resonance in Medicine; 3–9 May, 2008.
40. Lupo JM, Banerjee S, Hammond KE, et al. GRAPPA-based susceptibility-weighted imaging of normal volunteers and patients with brain tumor at 7 T. *Magn Reson Imaging*. 2009;27(4):480–488.
41. Studholme C, Hill D, Hawkes D. An overlap invariant entropy measure of 3D medical image alignment. *Pattern Recognit*. 1999; 32:71–86.
42. Wen PY, Macdonald DR, Reardon DA, et al. Updated response assessment criteria for high-grade gliomas: response assessment in neuro-oncology working group. *J Clin Oncol*. 2010;28(11): 1963–1972.
43. Therneau TM, Atkinson EJ. An in- troduction to recursive partitioning using the RPART routines. Technical Report. Mayo Foundation, 1997.
44. Sorensen AG, Batchelor TT, Wen PY, et al. Response criteria for glioma. *Nat Clin Pract Oncol*. 2008;5:634–644.
45. van den Bent MJ, Vogelbaum MA, Wen PY, Macdonald DR, Chang SM. End point assessment in gliomas: novel treatments limit usefulness of classical Macdonald's Criteria. *J Clin Oncol*. 2009;27: 2905–2908.